Simulated Effects of Idealized Laurentian Great Lakes on Regional and Large-Scale Climate*

BRENT M. LOFGREN

NOAA/Great Lakes Environmental Research Laboratory, Ann Arbor, Michigan

(Manuscript received 2 December 1996, in final form 17 March 1997)

ABSTRACT

Comparison is made between general circulation model (GCM) cases with and without the inclusion of idealized Great Lakes, in the form of four rectangular bodies of water, each occupying a single grid cell of the GCM at R30 resolution. The presence of idealized Great Lakes, as opposed to land, results in a phase shift in the annual cycle of latent and sensible heat flux. Very high upward sensible heat flux occurs over these idealized Great Lakes during the early winter. On the average over a region encompassing these idealized Great Lakes, evaporation and precipitation increase during the autumn and winter and decrease during the late spring and summer due to the lakes. Annual average water vapor flux convergence increases.

The Great Lakes also alter the meridional air temperature gradient. During the autumn and winter, the meridional temperature gradient is intensified to the north of the Great Lakes and diminished to the south. This intensifies the mean jet stream core and displaces it toward the north. This effect is reduced during the winter compared to the autumn because air temperature changes due to the lakes are unable to penetrate as deeply into the strongly stably stratified winter atmosphere. The increase in jet stream speed seems to increase synoptic wave activity to the northeast of the Great Lakes.

As an additional experimental case, a swamp surface (saturated surface with no thermal capacity) is used to represent the Great Lakes. In this case there is little effect on the thermal state of the surface and atmosphere and on the fluxes between them. However, there is increased evaporation during the late summer and early autumn and increased precipitation throughout the summer and autumn. Annual water vapor flux convergence in this experimental case is greater than in the case with no lakes.

1. Introduction

The Laurentian Great Lakes have a total surface area of approximately 245 000 km^2 and a total water volume of approximately 22 700 km^3. Thus they can have a large influence on local weather through their high thermal inertia. This inertia causes the surface temperature to exhibit greater persistence across the seasons than in the rest of North America. The lakes collect energy during the spring and summer and expend it over long periods during the fall and winter. Well-known short-term, localized phenomena resulting from this thermal inertia include lake-effect snow (e.g., Hjelmfelt 1990; Hjelmfelt and Braham 1983), lake breeze (e.g., Lyons and Cole 1976), and midlake cloud bands (Hjelmfelt 1990). Additionally, there are ''lake-aggregate'' thermal effects that can cause weakening, strengthening, or splitting of surface synoptic-scale systems (Sousounis and Shirer 1992; Sousounis and Fritsch 1994). Sousounis and Fritsch (1994) also noted remote effects of the Great Lakes in the form of different precipitation patterns over the Chesapeake Bay region and extending north.

However, all of the phenomena mentioned above are episodic in nature. In particular, the lake-aggregate effect is associated with synoptic-scale cold-air outbreaks. Also, Sousounis and Fritsch (1994) did not rigorously attribute the cyclogenesis over eastern North America to a particular mechanism, and a single case does not form a trend.

This leaves the question of how the Great Lakes affect the average climate for a given month or season. This paper considers the use of a general circulation model (GCM) to simulate the Great Lakes' effects on the budgets of water and energy in the surrounding area over climatic timescales. It will also deal with how the difference in surface energy fluxes due to the Great Lakes affect the long-term statistics of the atmospheric circulation. Using a GCM, we cannot hope to resolve the lake-effect snow, midlake cloud bands, or lake breeze. However, as in Sousounis and Fritsch (1994), lake-aggregate effects may be evident in geopotential heights, of which we are interested in the average and variability. These lake aggregates are likely to result both from the

* GLERL Contribution Number 1021.

Corresponding author address: Dr. Brent M. Lofgren, Great Lakes Environmental Research Laboratory, NOAA/ERL, 2205 Commonwealth Blvd., Ann Arbor, MI 48105-1593.
E-mail: lofgren@glerl.noaa.gov

linear combination of effects due to individual lakes and from nonlinear interactions among responses to individual lakes. On even larger scales, the Great Lakes may affect the thermal gradient that drives the jet stream.

Bonan (1995) has addressed a similar question using a different approach to including inland waters in a GCM. He separately calculated surface fluxes for land and water and weighted them according to the fraction of water in each grid box. His results showed a phase shift in the seasonal cycle of terms in the energy budget but indicated no significant changes in atmospheric circulation.

Another approach to this problem would be to use a regional atmospheric model with a smaller domain and finer resolution (Bates et al. 1993, 1995). This approach provides better representation of many relevant physical and dynamical mechanisms than a GCM, and we anticipate using this approach in the future. However, the GCM provides an entree to the use of a regional model, helping to identify some issues requiring investigation with a regional model or by direct observation. It may be able to identify phenomena of larger spatial scale than the domain of a regional model that result from forcing by the Great Lakes. It also runs faster than a regional model.

Section 2 describes the formulation of the atmospheric and lake models and the experimental cases. Section 3 gives the results from an experimental case using lakes with large thermal capacity. In section 4 we present the results from another experimental case in which the lakes are represented as surfaces with unlimited water availability but no thermal capacity. The major conclusions from this study, along with some caveats, are found in section 5.

2. Model formulation

a. General circulation model

The atmospheric model used here is a version of the Geophysical Fluid Dynamics Laboratory (GFDL) GCM. It uses the spectral transform method to solve the equations of motion, thermodynamical equation, and continuity equations of mass and moisture and to compute the vertical component of vorticity, horizontal divergence, temperature, surface pressure, and water vapor mixing ratio. The version used here has vertical resolution of nine unevenly spaced sigma layers, and uses rhomboidal-30 (R30) horizontal resolution (which transforms to a grid of 2.25° lat $\times$ 3.75° long). See section 5 for caveats regarding the horizontal resolution. The main features of the dynamical component of this model are described in Gordon and Stern (1982); more particular information on the spectral truncation and its effects are found in Manabe et al. (1979).

This GCM uses the realistic land surface albedo values given by CLIMAP (1981), while water surfaces are assigned a surface albedo dependent on latitude only. Sea surface temperatures are prescribed to observed climatological values. These runs also include a parameterization for wind drag by internal gravity waves forced by subgrid-scale topographic features of the surface (Broccoli and Manabe 1992).

The formulations of radiation, precipitation, moist convection, surface energy budget, water balance, and adjustment of surface albedo for snow are identical to the description given in Lofgren (1995). One salient feature for purposes of this study is the formulation of land surface temperature. It is determined diagnostically so that the inputs from solar radiation and downward longwave radiation are exactly balanced by the outputs due to upward longwave radiation and latent and sensible heat flux (i.e., the ground is considered to have no heat capacity). The surface water balance is simulated using a simple bucket model (Manabe 1969).

b. Lake model

A one-dimensional lake thermodynamic model was used for the experimental run. It is represented schematically in Fig. 1. The basic element of this model, rather than vertical levels, is daily inputs of heat. Given the lake surface temperature and near-surface conditions predicted by the atmospheric component of the model, the net energy flux at the lake surface is calculated at each time step and averaged over a 24-h period. Near-surface winds are also averaged over the same period, as an aging function. Daily inputs of heat of varying ages are superposed on one another.

The parameters that relate the aging of a daily dose of heat to the wind over the lake were calibrated by Croley and Assel (1994) separately for each lake. The model also differs among the lakes due to their mean depth. The lake model also includes a module to simulate ice formation (Croley and Assel 1994). When the water surface temperature reaches 0°C, ice is formed such that the latent heat of ice formation equals the energy lost due to the combination of net radiation, sensible heat flux, and latent heat flux. New ice can accumulate at the bottom or at the lateral edges of existing ice, thereby altering its thickness and fractional area.

Albedo and surface roughness are also altered by the presence of the lakes. The lakes have surface albedo of 0.08, while the corresponding land has surface albedo of approximately 0.15. All land is prescribed to have a surface roughness factor corresponding to a roughness length of about 48 mm, while water is assigned a roughness length of about 0.2 mm. When ice is formed, it retains a roughness length of about 0.2 mm and has a surface albedo of 0.55. The ice also inhibits direct transfer of sensible, latent, and longwave radiative heat fluxes between the underlying water and the atmosphere above.

Figure 2 illustrates the configuration of the idealized Great Lakes used for this study, and Table 1 gives the

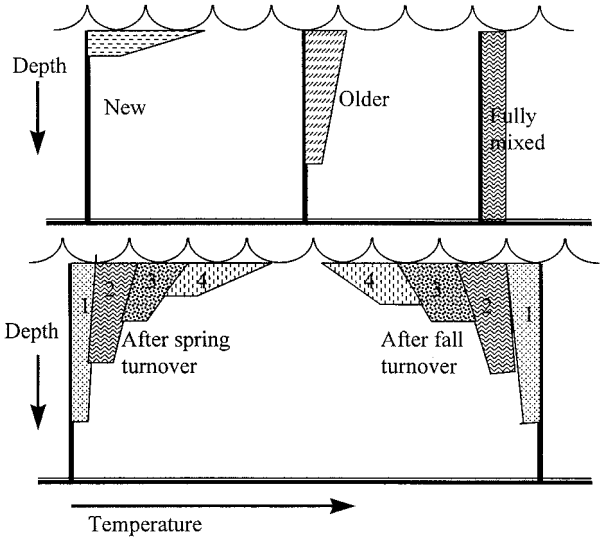

FIG. 1. Schematic diagram of the lake thermodynamics model used here (Croley 1989, 1992; Croley and Assel 1994). Depth is illustrated in the vertical, and temperature in the horizontal, with each vertical axis representing 3.98°C, the temperature of maximum density of freshwater. As illustrated at the top of the figure, a daily dose of heat newly input to the lake is concentrated near the surface. The wind speed integrated over the time since the dose of heat was input acts as an aging function, causing the heat to mix farther down into the lake, until it becomes homogeneously mixed to the bottom of the lake. The bottom part of the figure illustrates the temperature superposition scheme. As the water warms during the spring, it overturns and has a homogeneous temperature of 3.98°C at some time. Four days after this overturning (lower left), there are four daily doses of heat, each mixed downward to varying degrees, with the most recent occupying only a thin surface layer. When the lake begins losing energy, these daily doses of heat will be removed starting with the most recent, leading up to a fall turnover when all have been removed. After this, doses of negative heat accumulate (lower right).

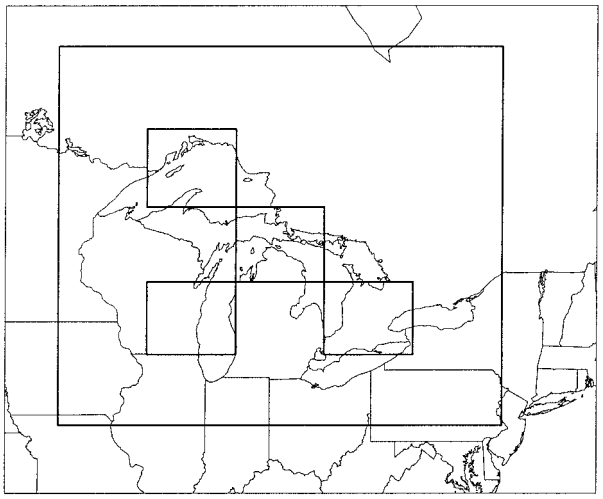

FIG. 2. A map of the Great Lakes region overlaid by the positions of the four idealized Great Lakes used in this study, along with a surrounding region used in subsequent analysis.

latitude–longitude coordinates of their centers. We use the correspondence shown in Table 1 between the actual lakes and the idealized lakes to assign the parameters governing thermal mixing as calibrated by Croley (1989, 1992) and Croley and Assel (1994).

Note in Fig. 2 that the size and location of Lake Superior is nearly correct. Lake Michigan is displaced to the south and west, Lake Huron to the north and west, and Lake Erie to the north. Lakes Michigan, Huron, and Erie each have their areas expanded. Lake Ontario is not present at all in order to get an approximate correspondence in total surface area between the actual Great Lakes and the model's idealized Great Lakes. The total surface area of the idealized lakes in this study is approximately 293 000 km^2, whereas the actual lakes have a total surface area of 245 000 km^2. The larger box in Fig. 2 defines a region that will be used later for areal averaging of various quantities.

c. Model experiments

The three model cases that were run for this study are called no lakes (NL), with lakes (WL), and swamp lakes (SL). In the NL simulation, the Great Lakes are depicted as land. This is the standard way of running the GFDL GCM at R30 resolution. The WL case has lakes inserted as shown in Fig. 2 and Table 1. The lakes differ from the land in terms of surface albedo, surface roughness, unlimited supply of water, and thermal capacity. Lake thermal capacity is formulated as stated in section 2b, whereas the land surfaces in the GCM have no thermal capacity. The SL case substitutes swamp lakes into the grid cells shown in Fig. 2 and Table 1. The swamp lakes differ from the land only in that the model assumes that they have an unlimited supply of water that keeps the ground evaporating at the potential rate. They are identical to land in terms of surface albedo, surface roughness, and thermal capacity.

In all cases, all air and land surface temperatures were initially set to 300 K and all soil moisture values were initially set to zero. In the NL and SL cases, the model was run for 22 yr; the first 2 yr were considered a spinup period, primarily for the soil moisture to reach a quasi-steady state, and their data were discarded. The results presented in this paper are taken from the following 20 yr. In the WL case, the lake temperatures (as represented by a series of daily heat inputs with associated aging functions) were initialized using an offline run of the lake model for the actual Great Lakes. A spinup period of 5 yr was then allowed for equilibration of the lake

TABLE 1. Position of the center of each grid cell representing an idealized lake.

Lake	Latitude	Longitude
Superior	48.38°N	90.00°W
Michigan	43.88°N	90.00°W
Huron	46.13°N	86.25°W
Erie	43.88°N	82.50°W

temperatures, and data from the subsequent 20 yr were used for analysis, for a total run of 25 yr.

The comparison of these three model cases will highlight the distinction between the effects of an unlimited local source of water and those of the long-term storage of heat.

3. Influence of full lakes (WL case)

a. Thermal state and fluxes

The way in which the lakes influence the atmosphere is highly dependent upon the evolution of their surface temperature. Figure 3 illustrates the simulated mean annual cycle of surface water temperatures for each of the four lakes. All share the feature that their temperature minimum is in late winter and their temperature maximum is in late summer. Lake Superior (Fig. 3a), because of its greater depth, tends to have temperature extrema late in the season more so than the others, and shallow Lake Erie (Fig. 3d) less so.

Also, each mean annual cycle has a sudden shift in the slope of the curve as the temperature crosses 4°C. This shift is smeared for all lakes because of averaging over the 20-yr period, but is most evident for Lake Superior (Fig. 3a). This shift is a result of the strong overturning before this temperature is reached and lack of overturning after it is reached (see section 2a and Fig. 1).

Figure 4 shows the seasonal dependence of fractional ice cover for the four lakes. Lake Erie (Fig. 4d), as the shallowest lake, cools and freezes most readily and so has the longest duration and highest peak ice coverage. Lake Huron (Fig. 4c) and, more so, Lake Superior (Fig. 4a), due to their depth, have a shorter duration and a lower maximum of ice cover. Lake Michigan (Fig. 4b) has the effects of its depth combined with its more southerly location (unrealistically far south) to give it the lowest maximum ice cover.

Figure 5 compares the surface temperature averaged over all four lake grid cells in the WL case with that over the same four grid cells in the NL case. Unlike Fig. 3, the lake surface temperature in Fig. 5 is an average of water and ice temperatures, weighted by the areal coverage of each. This makes temperatures below the freezing point possible for the lakes. The lakes have a lower temperature than the corresponding land during the spring and summer, up to about 5°C lower during May. They have higher temperatures during the autumn and winter, up to about 17°C higher during December. Annually averaged, the lakes are warmer than the land.

Surface energy fluxes over the lakes (Fig. 6) are the source of any forcing of the atmosphere by the surface. The net input of solar heat is much higher in the WL case than in the NL case during the spring and early summer. This is because of a combination of decreased cloudiness over the lakes and lower surface albedo. Net solar input is lower in WL during the autumn, when the lakes develop heavy low-level cloudiness.

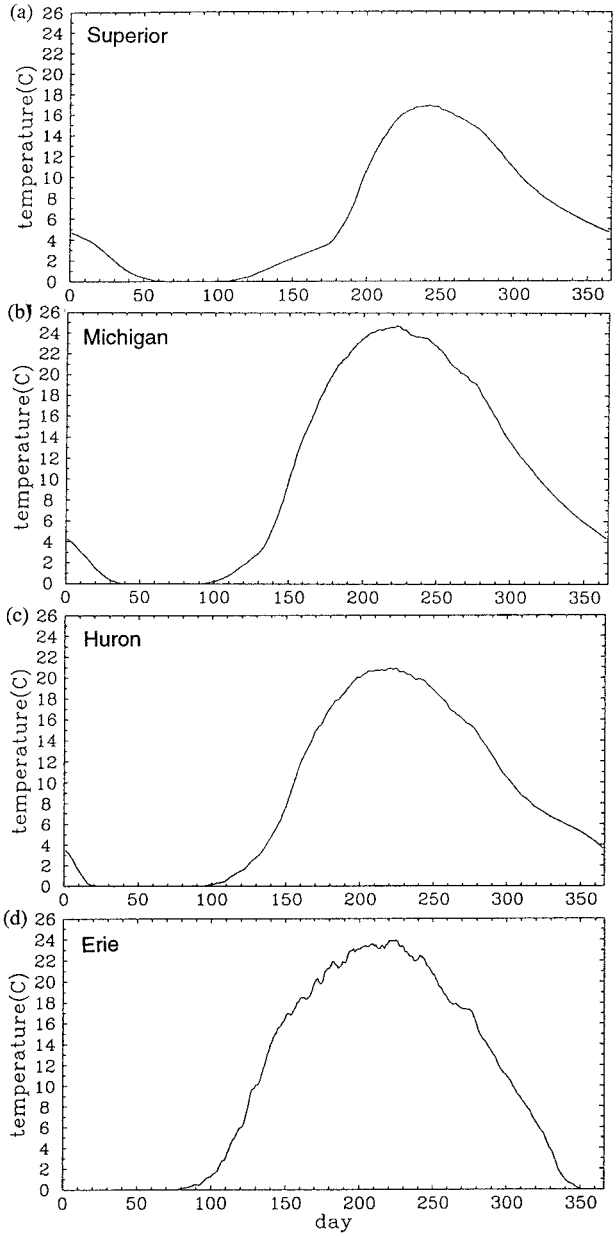

FIG. 3. Simulated mean annual cycle of surface temperature for (a) Lake Superior, (b) Lake Michigan, (c) Lake Huron, and (d) Lake Erie.

In the NL case, net outgoing longwave radiation has its peak value during September, when surface temperatures are still warm and the atmosphere is more cloud-free than earlier. Net outgoing longwave radiation remains more nearly constant in the WL case, in which higher surface temperatures than in the NL case during the autumn occur simultaneously with greater cloudiness.

The annual cycles of latent heat flux are out of phase

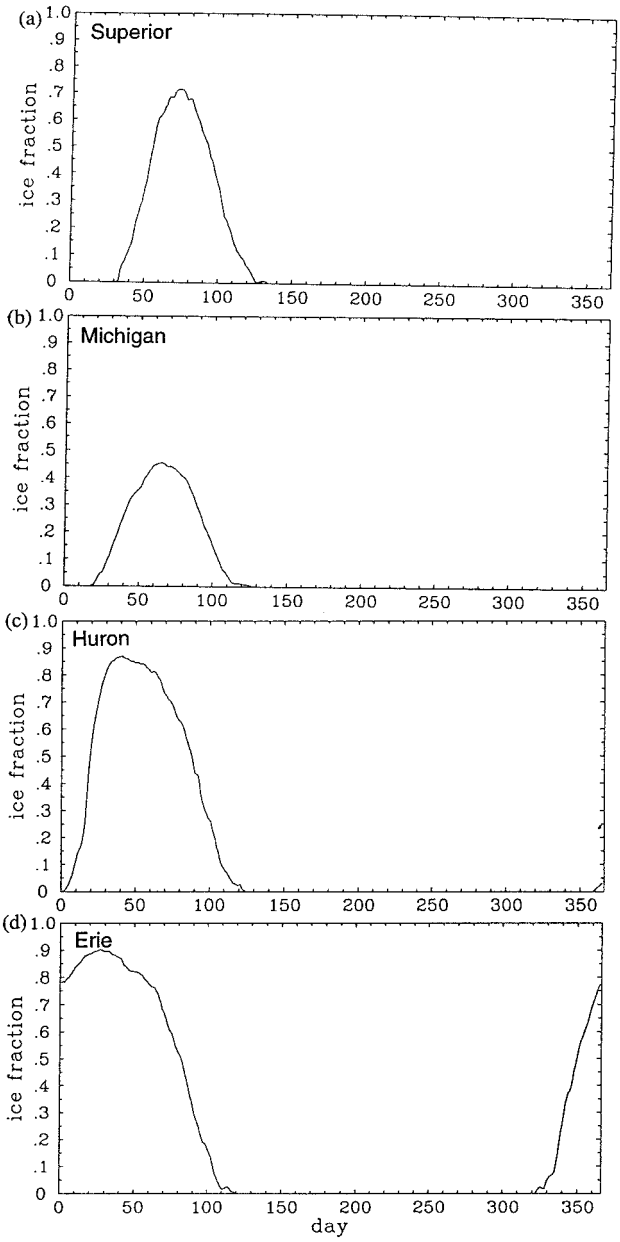

FIG. 4. Simulated mean annual cycle of fractional ice cover for (a) Lake Superior, (b) Lake Michigan, (c) Lake Huron, and (d) Lake Erie.

between the two cases. The NL case has its maximum value in July followed by a rapid decrease due both to the depletion of soil moisture and the reduced availability of energy. The WL case has its maximum in August followed by a gradual decrease. The WL case has latent heat fluxes far exceeding the NL case during the fall and into the winter, but falling short during the spring and early summer.

Sensible heat flux is more dramatically out of phase between the two cases. The NL case has maximum sensible heat flux during May through September, and negative values in November through March. The WL case has a remarkably large maximum in December and January, and a negative sensible heat flux in April through June. The outgoing sensible heat flux during November through January far exceeds the incoming solar radiation, dramatically demonstrating the hysteresis induced by the lakes' heat capacity.

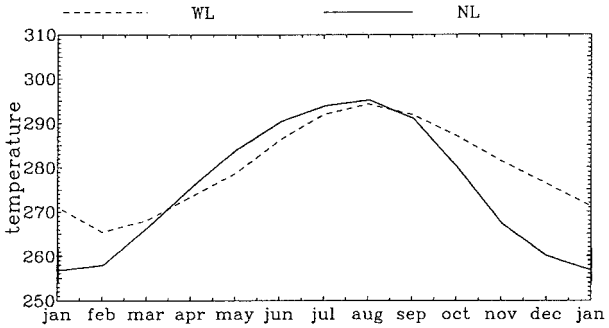

FIG. 5. Comparison of the annual cycle of mean surface temperature (in kelvins) averaged over the four lake grid cells in the WL case and over the same four grid cells (now land areas) in the NL case.

It is also important to note that in the WL case, the sensible heat flux continues to increase during the autumn, long after the latent heat flux has begun decreasing. This results in a Bowen ratio (sensible heat flux divided by latent heat flux) greater than 1 in December through February. These high Bowen ratios suggest that the boundary layer air maintains a nearly saturated state, while the lake continues to contribute more heat. The very high Bowen ratio during the winter seems to result

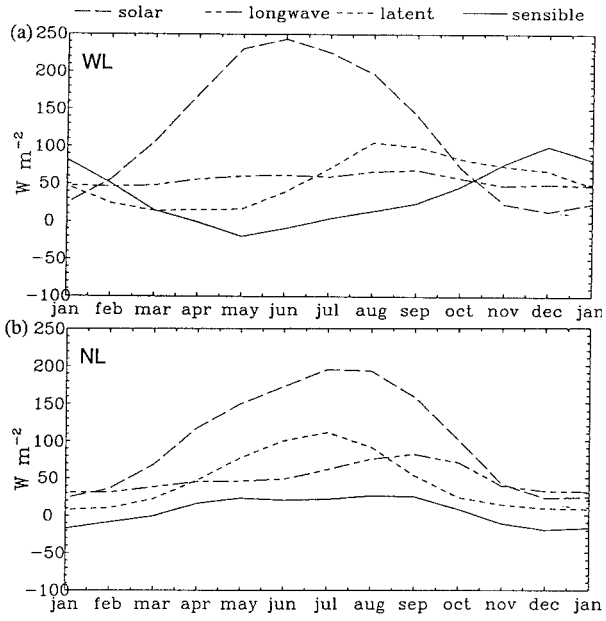

FIG. 6. Annual cycle of surface energy fluxes (net solar radiation, net longwave radiation, latent heat flux, and sensible heat flux) averaged over (a) the four lake grid cells in the WL case and (b) the same four grid cells in the NL case.

from a capping inversion at the top of the boundary layer, with associated clouds. This system radiates heat outward but allows only slow detrainment of moisture from the boundary layer. These heavy low-level clouds are unrealistically persistent, and this may be resulting in an exaggerated response in sensible heat flux at the expense of latent heat flux and longwave radiation.

The result that latent heat flux has its maximum value earlier than sensible heat flux agrees with the observationally based results of Pinsak and Rodgers (1981) for Lake Ontario and Schertzer (1987) for Lake Erie. However, they do not show the Bowen ratio exceeding 1. Schertzer (1978), looking at Lake Superior, found that both latent and sensible heat flux peak in February. The Bowen ratio exceeded 1 then, although not by as much as indicated by Fig. 6.

Figure 7 shows the precipitation in the NL case during the summer season (June–August) over northeastern North America, and the change that occurred due to the inclusion of the Great Lakes. The relative cold of the lake surfaces and suppression of sensible and latent heat flux (Figs. 5 and 6) stabilizes the atmospheric profile and suppresses convective precipitation over the lakes, although the decrease does not display a very high statistical significance. A similar decrease in precipitation over the lakes occurs during the spring season (not shown). Increased precipitation surrounding the lakes, particularly to the northwest, will be discussed in section 5.

Conversely, as shown in Fig. 8, the forcing due to the lakes during the winter decreases atmospheric stability, and the lakes become a strong direct source of water vapor. This results in enhanced precipitation, particularly over Lake Superior, to a lesser extent over Lakes Michigan and Huron, and only slightly over Lake Erie. During the fall season (not shown), precipitation increases more evenly over the four idealized lakes.

In looking at the total water balance, it is more useful to look at something more analogous to an entire drainage basin, which includes land along with water. Figure 9 displays quantities averaged over the larger rectangular area shown in Fig. 2, which we use for purposes of analysis, although it is much larger than the actual Great Lakes basin. In both the WL (Fig. 9a) and NL (not shown) cases, precipitation is less than evaporation during the summer, and exceeds evaporation (including sublimation) during the rest of the year. For the year as a whole, precipitation exceeds evaporation, indicating convergence of water vapor flux in the overlying atmosphere and nonnegative runoff from the region. The model enforces nonnegative runoff in the NL case, but not for the lakes in the WL case.

As in the results from the lakes alone (Fig. 6), the evaporation over the Great Lakes basin (Fig. 9b) decreases during the spring and early summer, and increases during the fall and winter due to the inclusion of the lakes. The changes in precipitation do not entirely follow these trends. The precipitation during the fall and winter increases by nearly as much as the evaporation.

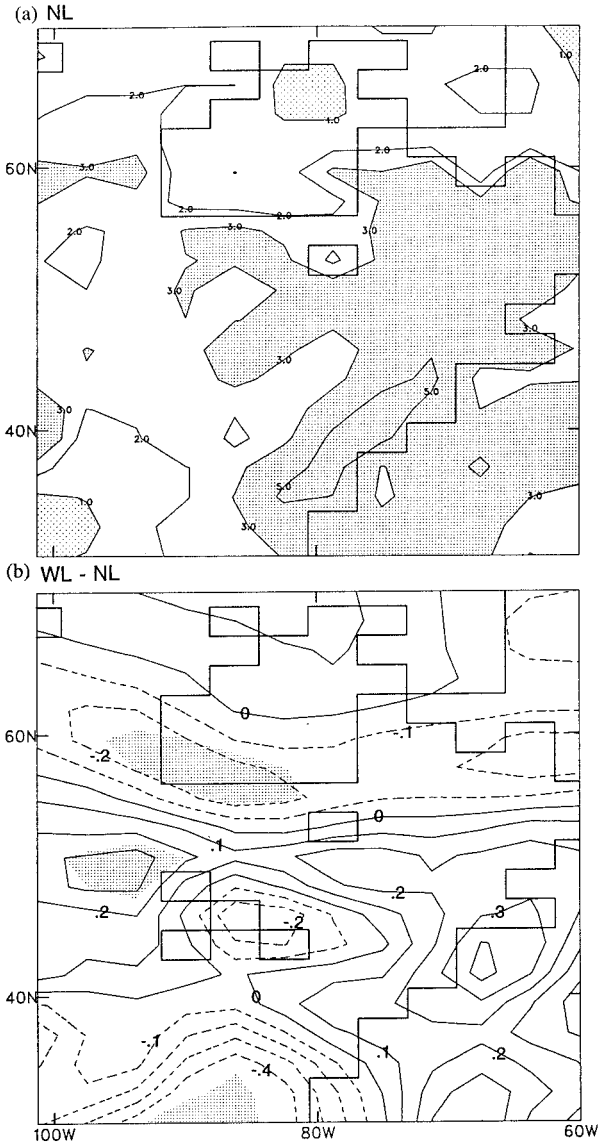

FIG. 7. Precipitation during June–August for (a) the NL case and (b) the WL case minus the NL case. The contours in (a) are 1, 2, 3, and 5 mm day^{-1}, with light shading for values less than 1 mm day^{-1} and heavy shading for values greater than 3 mm day^{-1}. In (b), the contour interval is 0.2 mm day^{-1}. In (b), a 1-2-1 spatial smoothing was applied in two dimensions, following which the Students t-test was applied to the seasonal means for each of the 20 yr; areas with statistical significance at the 95% level of confidence are shaded.

However, the decrease in evaporation during the spring and early summer is not accompanied by a decrease in precipitation over the analysis area as a whole. Thus, for the year as a whole, the inclusion of lakes results in an increase of precipitation minus evaporation of .049 mm day^{-1}. This corresponds to an increase in the convergence of atmospheric water vapor flux. This increase in flux convergence occurs partially over the lakes but more strongly over the surrounding land.

The precipitation minus evaporation was analyzed for

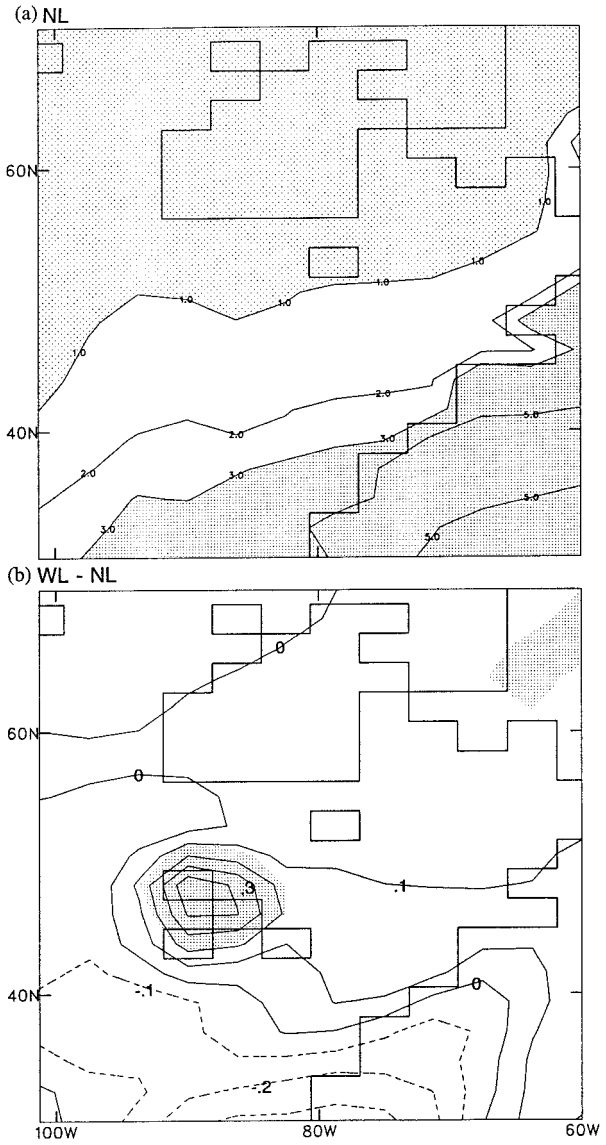

FIG. 8. As in Fig. 7 but for the months of December–February.

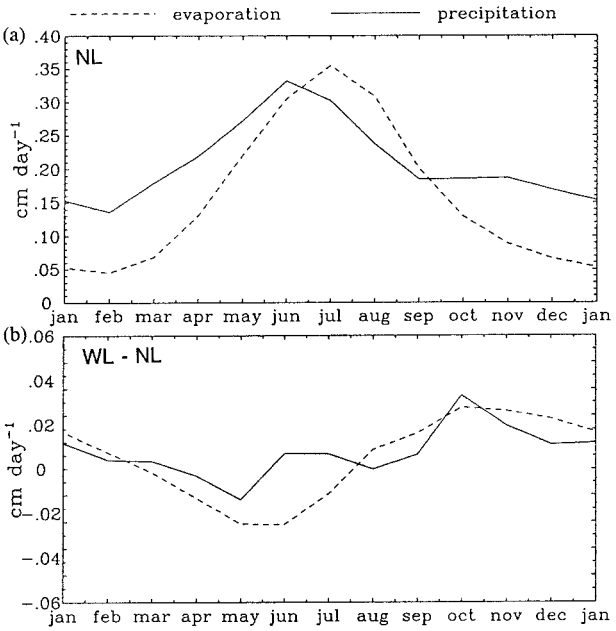

FIG. 9. Annual cycle of precipitation and evaporation for (a) the WL case and (b) the WL case minus the NL case, averaged over the region shown in Fig. 2.

statistical significance using the Wilcoxon test (Hollander and Wolfe 1973). The Wilcoxon test is nonparametric in that it assumes only that two distributions have the same shape, not what that shape is. It tests for a difference in their means by ranking the values of the sample sets from two distributions and comparing the sums of the ranks for each sample set. Using precipitation minus evaporation for individual years as input (assumed to be independent data), the increase in water vapor convergence is found to be significant at the 91% level of confidence

It may seem counterintuitive that the presence of an unlimited source of water would result in enhanced importation of water vapor from outside the basin. However, the seasonal effects are important here. In both the summer and winter, the Great Lakes become the site of temperature contrasts. They cool overlying air during the summer and force condensation; they inject water vapor into cold overlying air during the winter, again leading to condensation. The summer enhancement of water vapor convergence does not occur directly over the lakes, but is most strongly expressed just to the west. This is due at least partially to artificially very strong diffusion of air cooled by the lakes in this region (see section 5).

b. Mean zonal winds

The thermal wind equation for the atmosphere, based on geostrophic and hydrostatic assumptions along with the equation of state, says that

$$\frac{\partial u}{\partial z} = -\frac{g}{Tf}\frac{\partial T}{\partial y}, \tag{1}$$

where u is the zonal component of the wind, z is vertical distance, g is the gravitational constant, T is the air temperature, f is the Coriolis parameter, and y is meridional distance. Because of (1), we would expect that if the Great Lakes affect the meridional gradient of air temperature, they will also affect the zonal velocity of the jet stream.

Figure 10a shows a latitude-height cross section of the observed zonal wind component, averaged over the longitudes 60°–100°W and over the months of September–November (SON). Figure 10b shows the same quantity from the NL case of the model. The model's mean jet stream core is too weak and is slightly too far north in comparison to the observed data. There is also

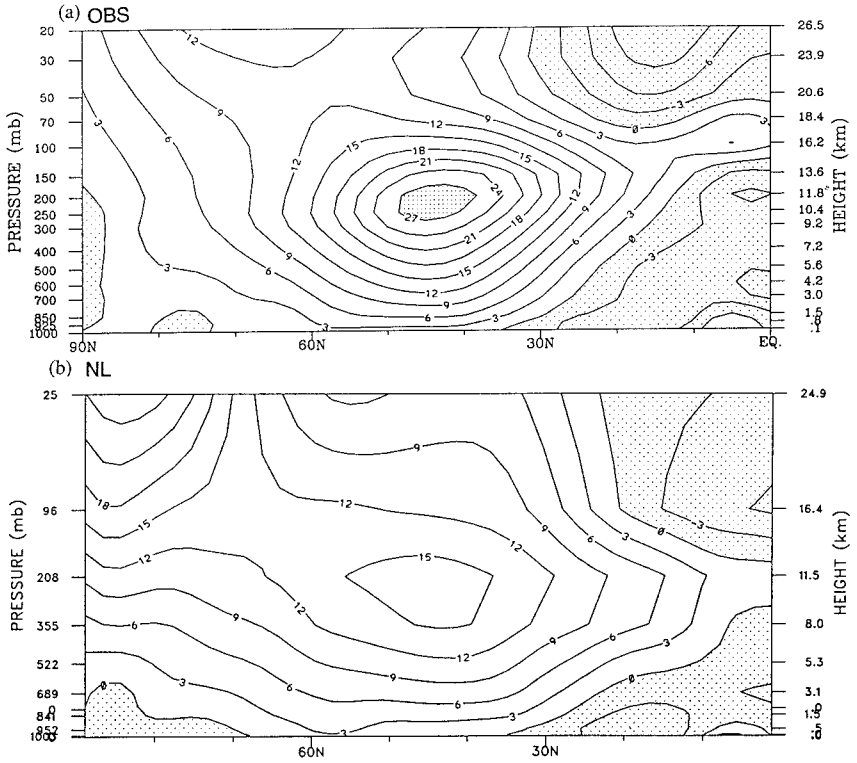

FIG. 10. (a) Latitude–height cross section of observed climatological zonal wind (Kalnay et al. 1996) averaged over the longitudes 60°–100°W and over the months of September–November, and (b) the same from the NL model case. The contour interval is 3 m s^{-1}. Values greater than 27 m s^{-1} have heavy shading and values less than 0 have light shading.

an excessively strong stratospheric jet in the polar region. According to Eq. (1), this implies that the strongest part of the north–south temperature gradient in the troposphere between 60° and 100°W is also too weak and located too far north.

Figure 11a shows how the SON zonal wind changes due to the inclusion of the idealized Great Lakes. There is a dipole of increased zonal wind to the north of the jet core and decreased to the south (cf. Fig. 10b). The net effect is that the Great Lakes act to intensify the mean jet stream core and shift it toward the north. The intensification puts the WL case in better agreement with the observations (Fig. 10a) than the NL case, but the northward shift reduces the agreement. Using as data points the means from individual SON seasons of zonal wind at sigma = 0.208 and 57°N, averaged between 60° and 100°W, the Wilcoxon test (Hollander and Wolfe 1973) shows that the increase in zonal wind speed is significant at the 92% level of confidence.

The changes in zonal wind are due almost entirely to the accompanying changes in the mean temperature structure, shown in Fig. 11b. By integrating Eq. (1) from the surface using the values of T shown in Fig. 11b and assuming zero wind at the surface, we can get a close approximation (not shown) of the change in zonal wind shown in Fig. 11a. The reason for weakening of the polar stratospheric jet and corresponding changes in the temperature profile are unknown.

The response in zonal mean wind during December–February (DJF) is quite different, however. Figure 12a shows the change in zonal winds due to the inclusion of idealized Great Lakes. This effect is considerably less than that noted in SON (Fig. 11a) and is significant at only an 81% level of confidence. Figure 12b shows the reason. Although the change in air temperature near the surface is more intense during DJF than during SON (Fig. 11b), its profile is much more shallow. If one were to vertically integrate (1), the effect on winds at jet stream level is less. The additional sensible heat output from the lakes is unable to penetrate to greater heights in the atmosphere because of the enhanced static stability of the free atmosphere during the winter. This inhibits vertical heat flux due to moist and dry convection and other mechanisms such as baroclinic waves. Recall that in section 3a we noted a cloud-capped boundary layer over the lakes at this time. The reason for intense cooling of the polar stratosphere and strengthening of the polar stratospheric jet are unknown.

There is enhanced variability in mean sea level pressure over and to the northeast of the lakes. This may be due to the combination of reduced static stability and increased jet stream velocity during SON and DJF, due

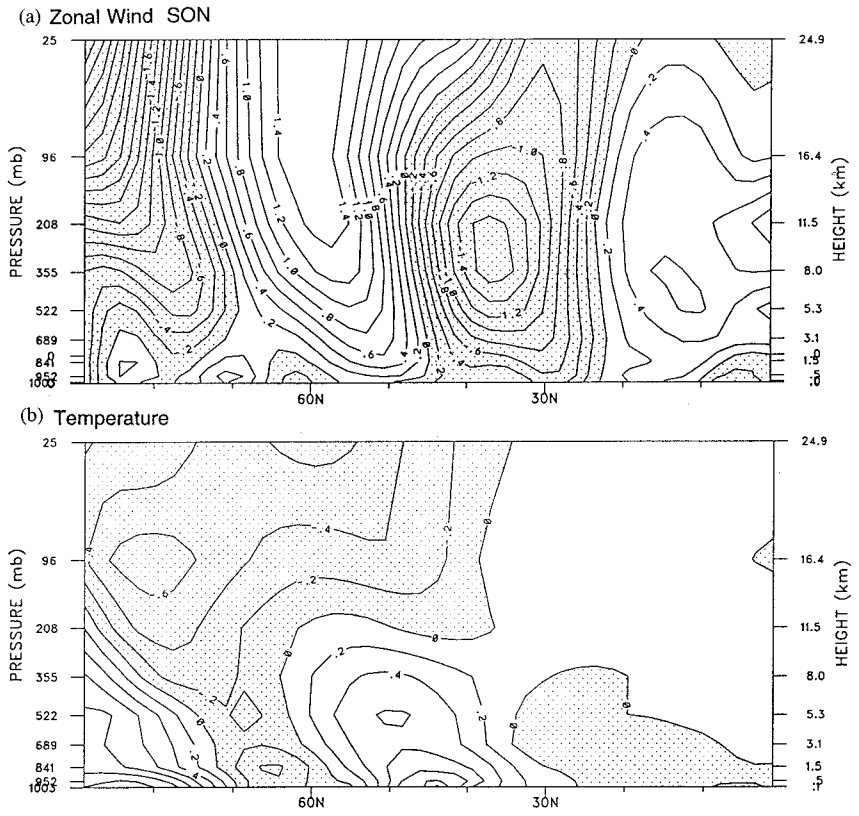

FIG. 11. Latitude–height cross section of the difference (WL case − NL case) during September–November in (a) zonal wind and (b) air temperature. In (a), the contour interval is 0.2 m s^{-1}. In (b) the contour interval is 0.2 K. In both, values less than 0 are shaded.

to the presence of the idealized Great Lakes, although the connection is rather tenuous. This effect is not illustrated here to conserve space and because the increase in variability is not significant at the 95% level of certainty at any point over northeastern North America. In apparent contradiction, Sousounis and Fritsch (1994) showed a reduction in extreme high pressure over and downstream of the Great Lakes during a cold air outbreak. Reproduction of this phenomenon multiple times would mean a reduction in pressure variability. The full theory of baroclinic instability and cyclogenesis in an environment of zonally varying zonal winds and vertically varying static stability is very complex, is beyond the scope of this paper, and is the subject of active current research (e.g., Branstator 1995).

4. Swamp lakes case

The swamp lakes case (SL) was undertaken to separate the effect of enhanced availability of water from that of enhanced thermal capacity in the lakes. Both were acting in the WL case, but in the SL case, the enhanced thermal capacity is absent. The lakes are treated like land in terms of thermal capacity, surface roughness, and surface albedo, but are assumed to be constantly saturated and evaporating at the potential rate.

Figure 13 shows that the swamp lakes have a small influence on surface temperature (cf. Fig. 5) during the late summer and early autumn, and almost none during the winter. The late summer and autumn are the times when the ground dries in the NL case, suppressing latent heat flux and forcing the surface temperature to increase in order to compensate. Under the prescribed saturation of the SL case, latent heat flux remains high throughout the summer, and surface temperatures remain relatively low. During the winter in the NL case, potential evaporation is reduced due to the reduced input of radiative energy, and soil moisture replenishes itself. Thus, during the winter, the NL case has evaporation near the (low) potential rate realized in the SL case, yielding a similar surface temperature.

Figure 14 displays mean precipitation and evaporation over the analysis area shown in Fig. 2. The unlimited supply of water from the swamp lakes causes an increase in evaporation during the late summer and early autumn. There is also an increase in precipitation that commences earlier in the summer. The net result is that the annual mean precipitation increases by a greater amount than the annual mean evaporation. This indicates enhanced convergence of atmospheric water vapor flux (significant at the 95% level of confidence). This shows that the additional evaporation from the swamp

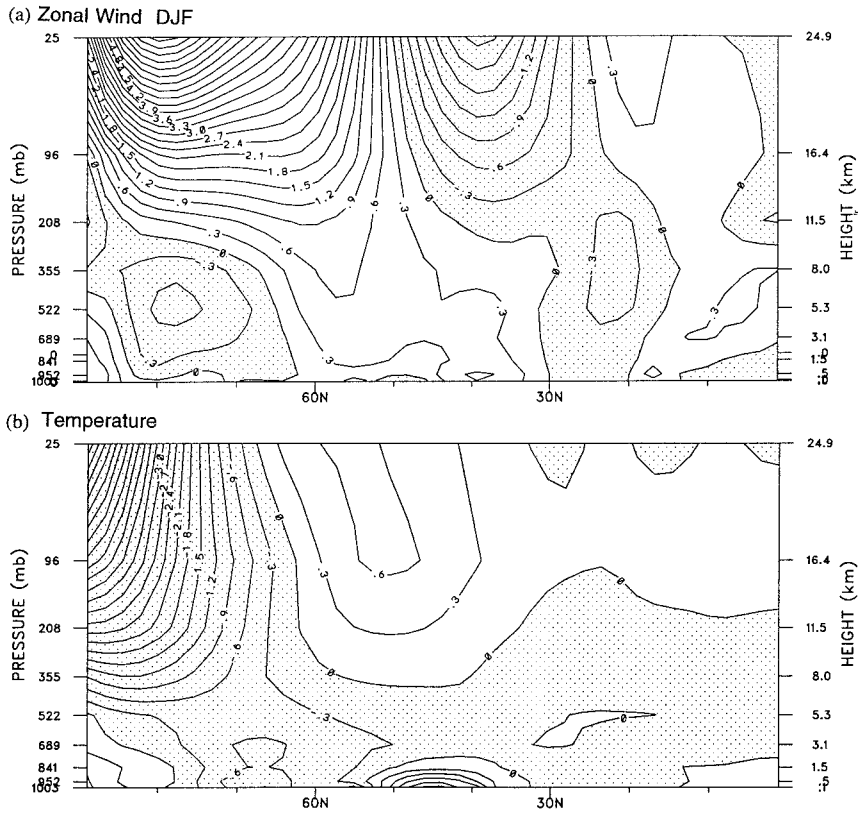

FIG. 12. Latitude–height cross section of the difference (WL case − NL case) during December–February in (a) zonal wind and (b) air temperature. In (a) the contour interval is 0.2 m s^{-1}. In (b) the contour interval is 0.3 K. In both, values less than 0 are shaded.

lakes, which is not large during June and July, is somehow ''seeding'' precipitation by attracting a larger influx of water vapor from outside the region.

5. Discussion and conclusions

The experiments discussed here are intended to illuminate some basic effects of the presence of the Great Lakes on hydrologic variables and atmospheric circulation at synoptic and larger spatial scales and over climatic timescales. Because of the idealized nature of the lakes used in these experiments and several caveats regarding the formulation of the model, the results given here are not to be taken as quantitatively exact answers.

The presence of idealized Great Lakes results in a phase shift in the annual cycle of latent and sensible heat flux from the lakes, in comparison to the land that would otherwise be there. The amplitude of the annual cycle of sensible heat flux also increases substantially.

Over a region encompassing the Great Lakes (see Fig.

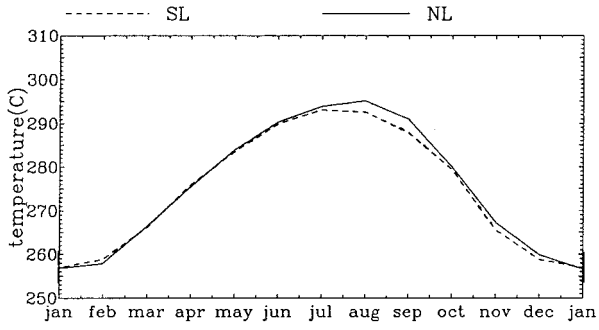

FIG. 13. Comparison of the annual cycle of mean surface temperature (in kelvins) averaged over the four lake grid cells in the SL case and over the same four grid cells (now land areas) in the NL case.

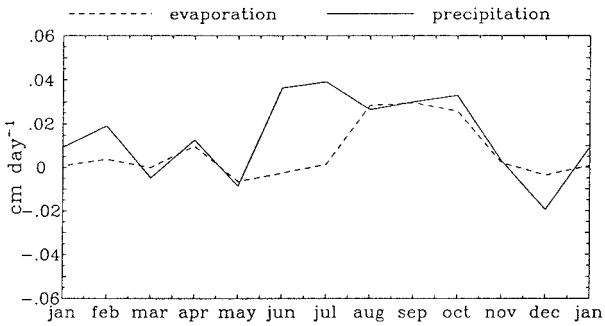

FIG. 14. Annual cycle of precipitation and evaporation for the SL case minus the NL case, averaged over the region shown in Fig. 2.

2), evaporation increases during the autumn and winter and decreases during the late spring and summer. During the autumn and winter, precipitation increases by a somewhat smaller amount than evaporation, and during the summer, precipitation decreases only slightly. In the annual average, precipitation minus evaporation increases indicating that there is increased convergence of water vapor flux over this region.

A caution that is relevant to this regional water balance, though, is that the spectral transform method uses different nominal resolutions for different processes and variables. Primary dynamical variables that are transformed between spectral and real space at each time step are vorticity, divergence, temperature, and pressure. The nominal resolution (one-half wavelength) of variables in spectral space is 3° lat × 6° long. Finer resolution (2.25° lat × 3.75° long) is required in the transform grid to prevent nonlinear aliasing when transforming back to spectral representation.

Figure 15 displays one implication of this. Figure 15a shows the change in sensible heat flux due to the inclusion of the Great Lakes during June–August. Sensible heat flux is calculated strictly under gridpoint representation, and major changes are limited to the individual grid points occupied by the idealized Great Lakes. However, the resulting change in air temperature has a very different pattern (Fig. 15b). The decrease in temperature has a strongly smoothed pattern, because the spectral transformation instantly removes features at the smallest scale represented by the grid. Spectral transformation has the effect of very strong diffusion on small-scale variations in air temperature and also wind and pressure.

Figure 15 shows that near-surface air temperature anomalies resulting from the Great Lakes are not as strongly localized as they might be in a finite-difference model. One effect of this is that the rapid diffusion of cold air during the summer from the lakes to the surrounding land areas leads to condensation over the surrounding land (see section 3a and Fig. 7). This occurs primarily on the upwind (western) side, where there is an influx of water vapor. In reality, this region would be largely unaffected by the lakes' temperature.

The change in meridional temperature gradient induced by the presence of idealized Great Lakes intensifies the mean jet stream core and displaces it toward the north during the autumn and, to a lesser extent, during the winter. The changes in air temperature due to the lakes are unable to penetrate as deeply into the strongly stably stratified winter atmosphere. The increase in jet stream speed combined with decreased static stability of the troposphere might play a role in increasing baroclinic wave activity to the northeast of the Great Lakes during the autumn and winter.

This is directly in contradiction to the results of Bonan (1995), who included inland waters in the NCAR Community Climate Model. His model accounted for surface state variables and fluxes separately for the respective

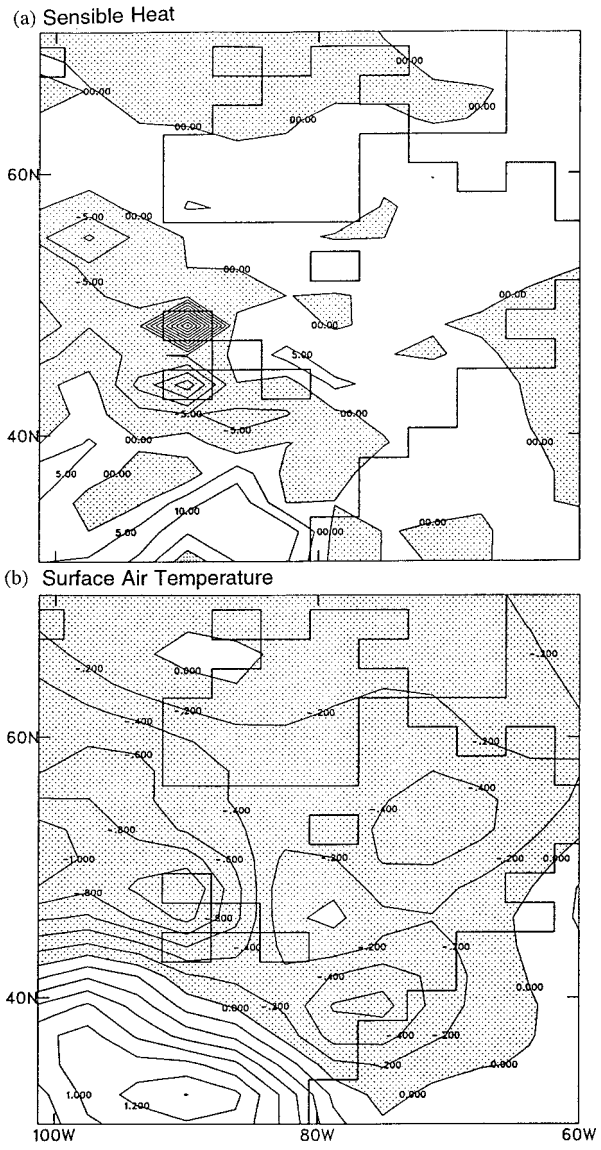

FIG. 15. Mean difference (WL case minus NL case) during June–August in (a) surface sensible heat flux and (b) air temperature at sigma = .99. In (a) the contour interval is 5 W m^{-2}, values greater than 20 W m^{-2} have heavy shading, and values less than 0 have light shading. In (b), the contour interval is 0.2 K and values less than 0 are shaded. No smoothing has been applied.

fractions of each grid space covered by land and water. Bonan showed the resulting changes in near-surface air temperature and some terms in the energy budget, but claimed that there was little resulting change in zonal circulation. One difference in treatment of the lakes was that whereas we used the thermal superposition method, assuming actual mean depths of the Great Lakes, Bonan used a simple vertical flux formulation and assumed that all lakes have a 50-m depth (Bonan 1996, personal communication).

In fact, some combination of the approach used here with that of Bonan (1995) may be better suited for taking

into account inland waters of the entire world. Bonan's use of fractional water cover over individual grid cells is probably more realistic than our strict land/water dichotomy for each cell. However, it still would not capture sub-grid-scale atmospheric variability due to lakes. For deep lakes such as Superior, Erie, and Huron, which characterize a large fraction of the area of a single grid cell, it is useful to have a model that takes their actual depth and seasonally dependent diffusion into account. In other regions, data may not be available for calibration of a model as in Croley and Assel (1994), making more useful a simple generic formulation, with perhaps some variation in depth. A single thermal reservoir may be the most appropriate model for many of the world's small, shallow lakes.

When the Great Lakes are represented as swamp with no heat capacity rather than water bodies with significant heat capacity, they behave very much like land during the winter. During the early summer, however, atmospheric water vapor convergence and precipitation intensify. During the late summer and early autumn, evaporation and precipitation are enhanced, with little change in atmospheric water vapor convergence.

It should also be considered that the results given here may be sensitive to the parameterization of moist convection. The GFDL GCM uses a very simple scheme to parameterize moist convection, and another treatment may yield different behavior in surface heat fluxes and atmospheric dynamics. Also, it was mentioned that the cloud cover over the Great Lakes during the winter is similar to a classic cloud-capped boundary layer. To simulate this phenomenon more accurately, it may be useful to replace the boundary-layer scheme used here, which uses prescribed mixing length, with a scheme that uses stability-dependent mixing. Improved vertical resolution would also be useful.

Acknowledgments. Thanks to Dr. S. Manabe for originally suggesting this experiment. Thanks to A. Broccoli, J. Lenters, and R. Stouffer for help in acquiring and running the GFDL GCM. Thanks to S. Manabe, R. Assel, and T. Croley for useful remarks on early versions of the manuscript, two anonymous reviewers for their remarks, and P. Sousounis for useful discussion.

REFERENCES

Bates, G. T., F. Giorgi, and S. W. Hostetler, 1993: Toward the simulation of the effects of the Great Lakes on regional climate. *Mon. Wea. Rev.,* **121,** 1373–1387.

——, S. W. Hostetler, and F. Giorgi, 1995: Two-year simulation of the Great Lakes region with a coupled modeling system. *Mon. Wea. Rev.,* **123,** 1505–1522.

Bonan, G. B., 1995: Sensitivity of a GCM simulation to inclusion of inland water surfaces. *J. Climate,* **8,** 2691–2704.

Branstator, G., 1995: Organization of storm track anomalies by recurring low-frequency circulation anomalies. *J. Atmos. Sci.,* **52,** 207–226.

Broccoli, A. J., and S. Manabe, 1992: The effects of orography on midlatitude Northern Hemisphere dry climates. *J. Climate,* **5,** 1181–1201.

CLIMAP, 1981: Seasonal reconstructions of the earth's surface at the last glacial maximum. Geological Society of America Map and Chart Series, MC-36, 18 pp. and 18 maps and microfiche. [Available from Geological Society of America, 3300 Penrose Place, P.O. Box 9410, Boulder, CO 80301-9140.]

Croley, T. E., II, 1989: Verifiable evaporation modeling on the Laurentian Great Lakes. *Water Resour. Res.,* **25,** 781–792.

——, 1992: Long-term heat storage in the Great Lakes. *Water Resour. Res.,* **28,** 69–81.

——, and R. A. Assel, 1994: A one-dimensional ice thermodynamics model for the Laurentian Great Lakes. *Water Resour. Res.,* **30,** 625–639.

Gordon, C. T., and W. F. Stern, 1982: A description of the GFDL global spectral model. *Mon. Wea. Rev.,* **110,** 625–644.

Hjelmfelt, M. R., 1990: Numerical study of the influence of environmental conditions on lake-effect snowstorms over Lake Michigan. *Mon. Wea. Rev.,* **118,** 138–150.

——, and R. R. Braham Jr., 1983: Numerical simulation of the airflow over Lake Michigan for a major lake-effect snow event. *Mon. Wea. Rev.,* **111,** 205–219.

Hollander, M., and D. A. Wolfe, 1973: *Nonparametric Statistical Methods.* Wiley, 503 pp.

Kalnay, E., and Coauthors, 1996: The NCEP/NCAR 40-year reanalysis project. *Bull. Amer. Meteor. Soc.,* **77,** 437–471.

Lofgren, B. M., 1995: Sensitivity of land-ocean circulations, precipitation, and soil moisture to perturbed land surface albedo. *J. Climate,* **8,** 2521–2542.

Lyons, W. A., and H. S. Cole, 1976: Photochemical oxidant transport: Mesoscale lake breeze and synoptic-scale aspects. *J. Appl. Meteor.,* **15,** 733–743.

Manabe, S., 1969: Climate and ocean circulation. Part I: The atmospheric circulation and the hydrology of the earth's surface. *Mon. Wea. Rev.,* **97,** 739–774.

——, D. G. Hahn, and J. L. Holloway Jr., 1979: Climate simulations with GFDL spectral models of the atmosphere: Effect of spectral truncation. Rep. of the JOC Study Conference on Climate Models: Performance, Intercomparison and Sensitivity Studies. GARP Publication Series 22, Vol. 1, 41–94, 1049 pp. [Available from World Meteorological Organization, Case Postale 2300, CH-1211 Geneva 2, Switzerland.]

Pinsak, A. P., and G. K. Rodgers, 1981: Energy balance. *IFYGL—The International Field Year for the Great Lakes,* E. J. Aubert and T. L. Richards, Eds., National Oceanic and Atmospheric Administration, 169–197.

Schertzer, W. M., 1978: Energy budget and monthly evaporation estimates for Lake Superior, 1973. *J. Great Lakes Res.,* **4,** 320–330.

——, 1987: Heat balance and heat storage estimates for Lake Erie, 1967 to 1982. *J. Great Lakes Res.,* **13,** 454–467.

Sousounis, P. J., and H. N. Shirer, 1992: Lake aggregate mesoscale disturbances. Part I: Linear analysis. *J. Atmos. Sci.,* **49,** 80–96.

——, and J. M. Fritsch, 1994: Lake-aggregate mesoscale disturbances. Part II: A case study of the effects on regional and synoptic-scale weather systems. *Bull. Amer. Meteor. Soc.,* **75,** 1793–1811.